






Perspective: Biomedical sensing and imaging with optical fibers—Innovation through convergence of science disciplines

Cite as: APL Photonics 3, 100902 (2018); <https://doi.org/10.1063/1.5040861>

Submitted: 21 May 2018 . Accepted: 21 August 2018 . Published Online: 10 September 2018

Jiawen Li , Heike Ebendorff-Heidepriem, Brant C. Gibson, Andrew D. Greentree , Mark R. Hutchinson , Peipei Jia, Roman Kostecki, Guozhen Liu, Antony Orth, Martin Ploschner, Erik P. Schartner, Stephen C. Warren-Smith , Kaixin Zhang, Georgios Tsiminis , and Ewa M. Goldys



View Online



Export Citation



CrossMark

ARTICLES YOU MAY BE INTERESTED IN

[Perspective: Wavefront shaping techniques for controlling multiple light scattering in biological tissues: Toward in vivo applications](#)

APL Photonics 3, 100901 (2018); <https://doi.org/10.1063/1.5033917>

[Perspective: Implantable optical systems for neuroscience research in behaving animal models—Current approaches and future directions](#)

APL Photonics 3, 120901 (2018); <https://doi.org/10.1063/1.5040256>

[Perspective: Coherent Raman scattering microscopy, the future is bright](#)

APL Photonics 3, 090901 (2018); <https://doi.org/10.1063/1.5040101>

AIP | Conference Proceedings

Get **30% off** all
print proceedings!

Enter Promotion Code **PDF30** at checkout



Perspective: Biomedical sensing and imaging with optical fibers—Innovation through convergence of science disciplines

Jiawen Li,^{1,2} Heike Ebendorff-Heidepriem,^{1,3,a} Brant C. Gibson,^{1,4,a} Andrew D. Greentree,^{1,4,a} Mark R. Hutchinson,^{1,2,a} Peipei Jia,^{1,3,a} Roman Kostecki,^{1,3,a} Guozhen Liu,^{1,5,6,a} Antony Orth,^{1,4,a} Martin Ploschner,^{7,a} Erik P. Schartner,^{1,3,a} Stephen C. Warren-Smith,^{1,3,8,a} Kaixin Zhang,^{1,7,a} Georgios Tsiminis,^{1,2,3,b} and Ewa M. Goldys^{1,5,b}

¹ARC Centre of Excellence for Nanoscale BioPhotonics (CNBP), Australia

²Institute for Photonics and Advanced Sensing (IPAS) and Adelaide Medical School, The University of Adelaide, Adelaide, South Australia 5005, Australia

³Institute for Photonics and Advanced Sensing (IPAS) and School of Physical Sciences, The University of Adelaide, Adelaide, South Australia 5005, Australia

⁴School of Science, RMIT University, Melbourne, Victoria 3001, Australia

⁵Graduate School of Biomedical Engineering, Faculty of Engineering, University of New South Wales, Sydney 2052, NSW, Australia

⁶International Joint Research Center for Intelligent Biosensor Technology and Health, College of Chemistry, Central China Normal University, Wuhan 430079, P. R. China

⁷Department of Physics and Astronomy, Macquarie University, Sydney, NSW 2109, Australia

⁸Leibniz Institute of Photonic Technology (IPHT Jena), Albert-Einstein-Straße 9, 07745 Jena, Germany

(Received 21 May 2018; accepted 21 August 2018; published online 10 September 2018)

The probing of physiological processes in living organisms is a grand challenge that requires bespoke analytical tools. Optical fiber probes offer a minimally invasive approach to report physiological signals from specific locations inside the body. This perspective article discusses a wide range of such fiber probes developed at the Australian Research Council Centre of Excellence for Nanoscale BioPhotonics. Our fiber platforms use a range of sensing modalities, including embedded nanodiamonds for magnetometry, interferometric fiber cavities for refractive index sensing, and tailored metal coatings for surface plasmon resonance sensing. Other fiber probes exploit molecularly sensitive Raman scattering or fluorescence where optical fibers have been combined with chemical and immunosensors. Fiber imaging probes based on interferometry and computational imaging are also discussed as emerging *in vivo* diagnostic devices. We provide examples to illustrate how the convergence of multiple scientific disciplines generates opportunities for the fiber probes to address key challenges in real-time *in vivo* diagnostics. These future fiber probes will enable the asking and answering of scientific questions that were never possible before. © 2018 Author(s). All article content, except where otherwise noted, is licensed under a Creative Commons Attribution (CC BY) license (<http://creativecommons.org/licenses/by/4.0/>). <https://doi.org/10.1063/1.5040861>

I. INTRODUCTION

The origins of health and disease arise from molecular events deep inside heterogeneous cellular structures in complex living organisms. Sensing and imaging of these events is an exciting but challenging area of scientific exploration.¹ This is because anatomically defined compartments such

^aH. Ebendorff-Heidepriem, B. C. Gibson, A. D. Greentree, M. R. Hutchinson, P. Jia, R. Kostecki, G. Liu, A. Orth, M. Ploschner, E. P. Schartner, S. C. Warren-Smith, and K. Zhang contributed equally to this work.

^bG. Tsiminis and E. M. Goldys contributed equally to this work.

^cAuthor to whom correspondence should be addressed: e.goldys@unsw.edu.au.



as the reproductive tract, the inside of blood vessels, and, most notably, defined nuclei of the brain and spinal cord are notoriously difficult to access in a non-invasive or minimally invasive way. As a result, many fundamental physiological events and processes cannot be fully understood. Our understanding of such processes must often be reconstructed from isolated snapshots in time in parallel experiments, owing to the difficulty to conduct longitudinal repeated measurements, where a single individual is monitored over a longer period.² This leads to fragmented understanding of the molecular events and pathways, infrequently replicated studies, and limits our ability to design medical interventions.

The breakthroughs in imaging and sensing fiber probes cannot be made in isolation from the biomedical disciplines; transformative outcomes can only be enabled collaboratively through a convergence of scientific disciplines. Inspired by the motivations from neuroscience, reproductive, and cardiovascular health, researchers in the Australian Research Council Centre of Excellence for Nanoscale BioPhotonics have been developing new imaging and sensing technologies suitable for *in vivo* use. These advances in technology must meet a range of stringent requirements, such as the ability to sense and/or image: (i) in ultrasmall volumes; (ii) in spatially defined location in the body; (iii) *in vivo*, in living, naturally behaving animals; (iv) at the relevant time scale, including in real-time; (v) with high sensitivity, selectivity, and specificity in a matrix sample environment; (vi) by using deployable devices whenever required. Optical fiber probes are capable of simultaneously meeting most of these conditions, and therefore they are set to play a special role in *in vivo* sensing and imaging.

Optical fiber probes are a mature technology with numerous research and industry applications.^{3,4} These applications typically exploit the immunity of optical fibers to electromagnetic interference, small weight, large bandwidth, very long interaction length, and related capability of sensing over large distances, and the feasibility of multiplexed or distributed sensing.⁵⁻⁷ The key enabling features of optical fibers for *in vivo* sensing and imaging are their small footprint and their inert glass composition, allowing for non-invasive or minimally invasive surgical implantation and non-destructive probing deep within the tissue. Critically, such light-based imaging and sensing technologies lend themselves to the repeated measurement of molecular events in defined anatomical locations in behaving preclinical models.

Building on this foundation, we have designed a range of optical fiber sensing and imaging platforms which offer unique “windows to the body.”^{2,8-30} Specific modalities have been chosen for defined uses owing to their unique characteristics for each biomedical application. For example, magnetically sensitive optical fibers (Sec. II A) pave the way to field-deployable magneto-endoscopy and magnetoencephalography for mapping brain activity. Optical fiber sensors based on the principles of interferometry (Sec. II B) and Surface Plasmon Resonance (Sec. II C) quantify biomedical analytes by detecting changes in the refractive index. The molecular specificity in these approaches is derived from the recognition molecules such as antibodies and/or aptamers used to specifically target the chosen analytes. They make it possible to reduce the sensing area (down to tens of μm), so that molecular information on a local scale can be obtained, and yet with a signal to noise ratio sufficient to capture specific rare and rapid molecular events. By contrast, by detecting a fingerprint spectrum, such as that of chemical bonds derived from Raman fiber probes (Sec. II D), a level of molecularly specific sensing *in vitro* and *in vivo* can be achieved in a true label-free fashion.³¹ Fluorescence-based fiber sensors (Sec. II E) typically utilize molecular or nanomaterial probes on the surface of the fiber core. These types of surface modified fibers can achieve molecularly specific biochemical sensing, for example, of metal ions or biomarkers, as well as sense other physiologically important parameters, such as the temperature, deep in the body *in vivo*. In the special case of temperature sensing, lanthanide ions offer convenient real-time temperature detection, and using this approach, we have been able to demonstrate temperature sensors to measure the brain temperature *in vivo* (Sec. II F). The standard approach of immunosensing is not yet compatible with real time sensing; however, when integrated with optical fibers, it can be used for repeated spatially localized measurements. We demonstrated this by detecting key immune signaling molecules called cytokines, *in vivo* in the brain² (Sec. II G).

Optical fiber platforms also support imaging modalities important for *in vivo* bioanalysis. The interferometry-based imaging with a single mode fiber can achieve depth-resolved imaging

in vivo with a spatial resolution of 1-30 μm ^{32,33} (Sec. III A). A multimode fiber combined with holographic and computational techniques can enable depth-resolved imaging with an even higher spatial resolution ($<1 \mu\text{m}$), as demonstrated in *ex vivo* settings (Sec. III B). A further computational technique that significantly improves image sharpness for widely used optical fiber bundle endoscopes, is also reviewed here. These examples illustrate how optical fiber technology can be adapted for the demands of current and future sensing and imaging *in vivo*.

II. SENSING PLATFORMS

A. Magnetically sensitive fibers through nanodiamond doping

We developed optical fiber materials doped with nanodiamonds (NDs) to produce intrinsically magnetically sensitive optical fibers.^{14,28,34,35} They owe their sensitivity to the magnetic field at ambient conditions and within a nano-scaled sensing volume to the negatively charged nitrogen vacancy color centers (NVs) in NDs.^{36,37} Magnetic field sensing with NVs is based on optically detected magnetic resonance (ODMR),³⁸ where particulars of the spin conserving and spin non-conserving excitation/fluorescence pathways give rise to a differential brightness between the ground states of the spin one centre.³⁸ This change in brightness can be read out at room temperature. The energy levels shift with the external magnetic, and these shifts are determined using an external microwave field [Fig. 1(a)]. Unlike conventional confocal readout, such magnetically sensitive optical fibers offer small-size, mechanically stable collection optics and integration with mature photonic technologies,¹⁴ paving the way for sensing in difficult to reach places, including *in vivo* magneto-endoscopy. Recent work has considered positioning NDs on the surface of fiber tips and tapers for coupling the NV emission to the near-field or evanescent field of optical fibers.^{39–43} We have demonstrated an alternative, where the NV emission was coupled to fiber modes by embedding NDs in the fiber core material.^{14,34,35}

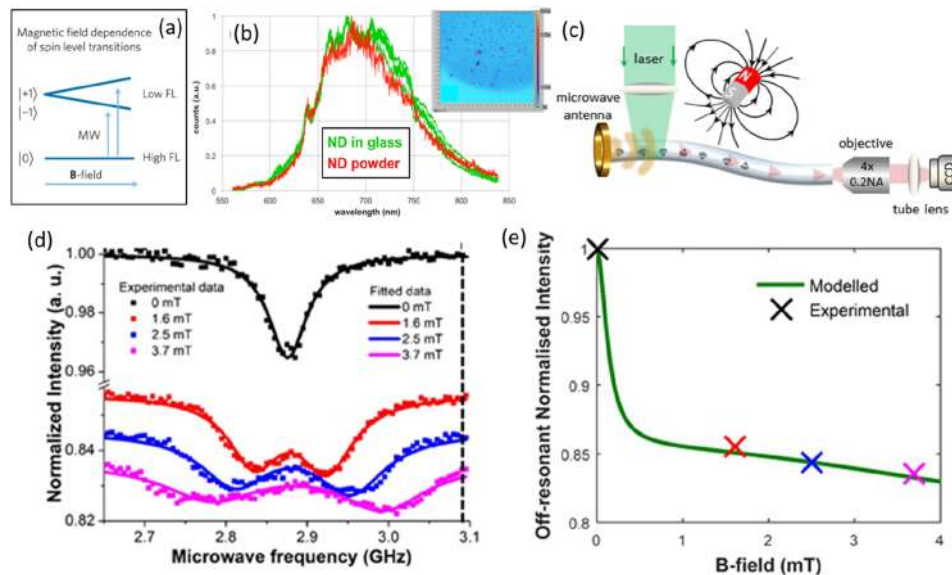


FIG. 1. Key characteristics of the nanodiamond-doped tellurite glass material and fiber. (a) Magnetic field dependence of spin level transitions of NV. (b) Fluorescence spectra of ND powder and ND embedded in the fiber; the inset shows the confocal microscopy image of emitters in the fiber. (c) Experimental setup for ODMR measurements. (d) The evolution of ODMR spectra at increasing external magnetic field. (e) Theoretical model of the off-resonance NV fluorescence intensity versus magnetic field and experimentally determined data from the nanodiamond-doped fiber. Reprinted with permission from Ruan *et al.*, *Opt. Mater. Express* **5**(1), 73 (2015). Copyright 2015 Author(s), licensed under a Creative Commons Attribution 4.0 License and Ruan *et al.*, *Sci. Rep.* **8**(1), 1268 (2018). Copyright 2018 Author(s), licensed under a Creative Commons Attribution 4.0 License.

Direct incorporation of diamond into the glass material is challenging. Most glasses melt at high temperatures that are incompatible with NDs, which oxidise at around 600 °C in an oxygen ambient and even in a vacuum at around 900 °C convert spontaneously to graphite. Additionally, mismatches between the relatively high refractive index of diamond ($n = 2.4$), compared to most optical fiber glasses ($n \sim 1.5$), result in significant scattering from the diamond/glass interface. We selected tellurite glass for embedding NDs since it can be processed at <700 °C, exhibiting high transmission in the visible wavelength range of NV excitation and emission and a high refractive index of 2.0.^{14,34,35} To minimize the temperature and time of exposure of NDs to the hot glass melt, we employed a two-step melting procedure, where first the glass batch was melted without ND at a high temperature, and then the NDs were dispersed in the melt at a lower temperature.³⁵ The obtained billet was then further processed at lower temperatures (400 °C) to fabricate an unstructured ND doped fiber.¹⁴ Optimization of glass composition and melting conditions resulted in ND-doped fibers with sufficiently low loss for practical applications and fluorescence comparable to the as-received ND [Fig. 1(b)].¹⁴

A low-loss nanodiamond-doped tellurite fiber, with estimated 0.7 ppm of ND, was used to investigate the magnetic field sensitivity via ODMR using side excitation and longitudinal collection [Fig. 1(c)].²⁸ The ODMR showed increasing Zeeman splitting with increasing magnetic field [Fig. 1(d)]. The $\sim 3\%$ contrast of the ODMR signal of the NV ensembles in NDs embedded in glass is comparable to conventional NV ensemble systems.⁴⁴ The broader linewidth of the ODMR signal of our fiber relative to NV ensembles in bulk diamond⁴⁵ indicates that several NDs were probed within the excitation volume [Fig. 1(a)]. Combining the ODMR signal linewidth, contrast, and photon count allowed us to estimate the magnetic field sensitivity at ~ 11 $\mu\text{T}/\sqrt{\text{Hz}}$, which is comparable to that of NDs placed on the fiber taper surfaces.^{46,47} When the magnetic field is not aligned with the NV quantization axis, the field induces spin flips even without an RF field, and hence the NV ensemble fluorescence shows a magnetic field response even at the RF-free conditions [Fig. 1(e)]. Although less sensitive than ODMR, this response greatly reduces the experimental complexity.

The intrinsically magnetically sensitive diamond-glass hybrid fibers enable a new generation of robust magnetic field sensors. As the entire fiber length and cross section contains NDs, exciting different positions along the fiber offers the possibility of detection of magnetic field gradients. Embedding of NDs in glass protects them from dislocation and simplifies the measurement compared with NDs placed at the fiber surface. The magnetic field sensitivity can be enhanced by reducing fiber loss while increasing ND concentration. Finally, embedding ND in glasses with superior thermal and mechanical stability relative to tellurite glass would improve the ruggedness of fiber sensors with intrinsic magnetic sensitivity.

B. Interferometric sensing

Chemical sensing using interferometry is based on accurate measurements of the local refractive index, which is increased upon binding of target analytes. Interferometry is highly compatible with optical fibers, and essentially any form of interferometer can be implemented in an optical fiber configuration, through a judicious choice of fiber design, tapering, splicing, grating inscription, and micro-machining.^{48,49} Figure 2(a) shows an example of a fiber-based Mach-Zehnder interferometer built in our centre from an exposed-core microstructured optical fiber spliced between two standard single-mode fibers. The excitation of higher order modes within the fiber is sensitive to binding events taking place on the surface of fiber core via the evanescent field.¹² While the wavelength sensitivity, 667 nm/RIU, is lower than similar surface plasmon resonance based fiber sensors, which can reach multiple times this value,⁵⁰ the sensor exhibits high stability as there are no metal coatings. The sensor has a detection limit the order of 10^{-6} RIU, and using it, we demonstrated the detection of proteins (e.g., streptavidin) at concentrations as low as 3.8 μM .

Ultrasmall in-fiber interferometry devices can be achieved through the addition of a small indentation to the fiber that acts as a cavity [Fig. 2(b)].⁵¹ Devices with cavities as small as 2.8 μm have been fabricated using focused ion beam milling. These sensors operate via interference between the two reflecting beams from each interface, forming a low-finesse Fabry-Perot cavity. Tracking

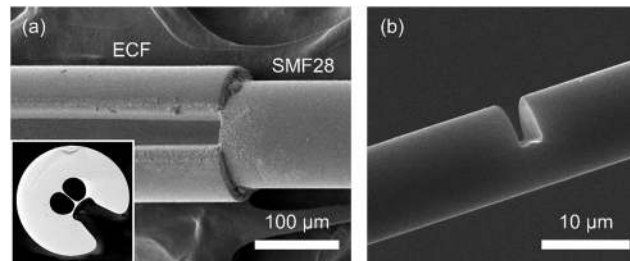


FIG. 2. Scanning electron microscope (SEM) images of interferometric optical fiber sensors. (a) Exposed-core microstructured optical fiber (ECF) spliced to the standard single mode fiber (SMF28). Inset: cross section of the ECF (160 μm outer diameter). (b) A tapered optical fiber with a 2.8 μm cavity formed by focused ion beam milling.

the interference fringes using Fourier techniques enables the sensitive measurement of refractive index changes and thin-layer coatings. Sensitivity in the order of 400 nm/RIU was achieved, and the detection of thin (1-2 nm) coatings of polyelectrolytes demonstrated the feasibility of biochemical sensing.⁵¹ The small spatial scale of the sensor offers potential opportunities to perform intracellular measurements (the cell size is in the order of 10 μm). Alternatively, cavities can be written into exposed-core fibers, which provide a platform for biochemical sensing that is physically more robust than fiber tapers.⁵² We anticipate that future work in fiber integrated interferometric sensors will likely focus on application-specific implementation, and increasing the ability of such sensors to perform simultaneous measurements of multiple parameters, such as the temperature and refractive index.⁵³

C. Surface plasmon resonance sensing

Surface plasmon resonances (SPRs) are collective electronic excitations localized at metal surfaces that are sensitive to refractive index variation at the interface with the surrounding medium. In SPR sensing, molecular targets are captured at metal surfaces by recognition molecules (antibodies, nanobodies, aptamers, enzymes, ligands, peptides, lectins, etc.) which then interact with the SPRs. Optical fibers offer an intrinsic advantage for SPR sensing due to the generally straightforward coupling of light to plasmonic nanomaterials (such as gold nanoparticles or nanorods) deposited over the length of the fiber.⁵⁴ It is also possible to deposit active plasmonic structures on optical fiber tips; these are of particular utility in remote sensing and spectroscopy.⁵⁵

Two general strategies can be deployed to fabricate plasmonic nanostructures on fiber facets. *In situ* fabrication involves direct writing of structures onto the fiber, for example, by electron-beam lithography,⁵⁶ focused ion beam milling, two-photon direct laser writing, or interference lithography.⁵⁵ An alternative strategy is to fabricate the nanostructures on a planar substrate and then transfer them to the fiber tips.^{57,58} To this aim, we used an epoxy as an adhesive layer, after metal deposition on the template; see Fig. 3(a).^{16,59} This enhances adhesion, enabling our plasmonic sensor to support long-term biosensing applications. Using this approach, we demonstrated a plasmonic fiber simultaneously implementing multimode refractive index sensing (transmission and reflection), achieving 595 nm/RIU sensitivity, narrow linewidth (6.6 nm), and high figure of merit (sensitivity/linewidth = 60.7), which are both among the best reported values for nanostructure SPR sensors.¹⁶ In combination with a custom-made flow cell, this plasmonic fiber has been used to demonstrate a real-time immunoassay of bovine serum albumin [BSA, Fig. 3(b)].¹⁶

In order to enable high-throughput fabrication of plasmonic fiber sensors, we developed a direct nanoimprint technique.⁶⁰ In this single-step technique, the optical fiber tips are imprinted against a mold with nanostructures at elevated temperatures [Fig. 4(a)]. This simple method does not require the photolithography used in previous fiber-imprinting techniques. Hundreds of fibers can be shaped simultaneously within minutes; hence, the technique is suitable for high volume production. Various nanostructure arrays can be imprinted into plastic optical fiber tips with high precision and quality [Figs. 4(c)–4(e)], which can then be transformed into plasmonic crystals through metallization [Fig. 4(b)]. By controlling pressure, it is possible to adjust the imprint depth and thereby modulate plasmonic coupling between resonances at different levels of the imprinted structures. We also

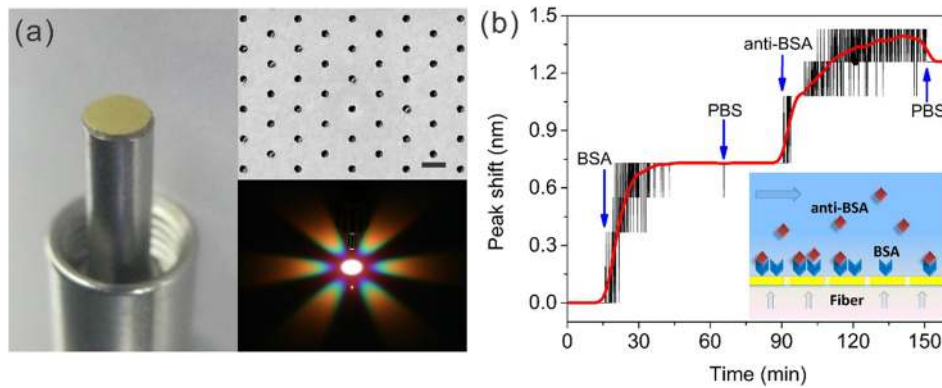


FIG. 3. Plasmonic optical fibers suitable for SPR biosensing.¹⁶ (a) Photographs of an optical fiber with a gold nanohole array on the tip (left); SEM of the nanohole array (top-right) and far-field diffraction pattern (bottom-right). (b) Label-free real-time biosensing of BSA using a plasmonic optical fiber. Reprinted with permission from Jia *et al.*, ACS Sens. **1**(8), 1078 (2016). Copyright 2016 Author(s), licensed under a Creative Commons Attribution 4.0 License.

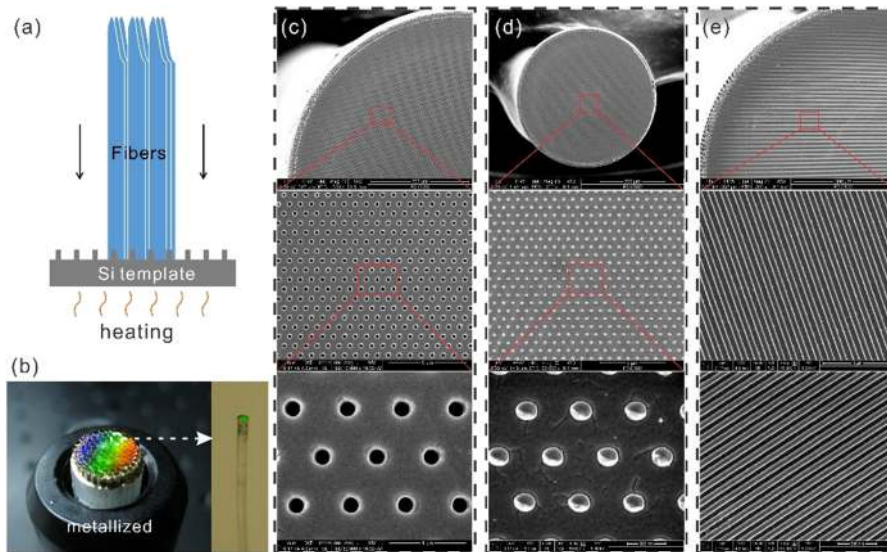


FIG. 4. Direct optical fiber nanoimprint. (a) Diagram of batch imprinting of optical fibers against pre-patterned Si templates. (b) A bundle of imprinted fibers after metal deposition. [(c)–(e)] SEM of various arrays of nano-holes, dots, and slits imprinted on the plastic optical fiber facets.

demonstrated on-fiber polarizers by imprinting nanoslits on fiber tips. This low-cost nanoimprint technique makes it possible to fabricate cheap disposable plasmonic optical fiber devices for biological replication studies.

D. Raman fiber sensing

Raman spectroscopy is a label-free technique which is increasingly used in biomedical applications.^{25,61–63} The Raman signature of a chemical species corresponds to the vibrational modes of its chemical bonds, which can be directly identified.⁶⁴ The measurement of Raman spectra at specific locations *in vivo* requires a probe delivering the excitation light and collecting the Raman signal, usually from the fiber tip. As the Raman effect is inherently weak, specially designed probes have been developed to yield improved signal-to-noise ratios.⁶⁴ One approach is to utilize the unique properties of microstructured optical fibers to create extended light-sample overlaps over the fiber length to enhance the resulting optical signal, for example, by using suspended core optical fibers

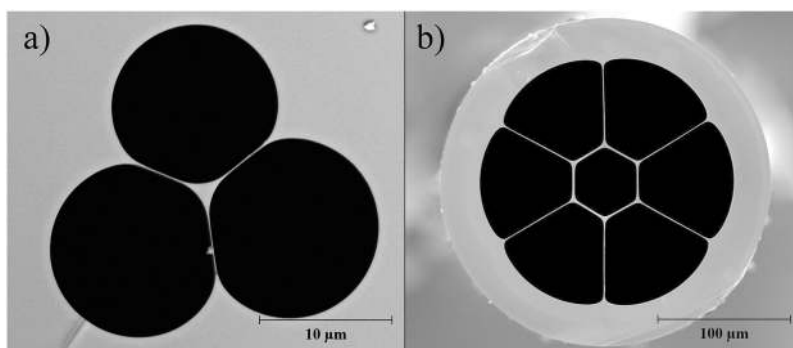


FIG. 5. Scanning electron micrographs of (a) a suspended core optical fiber used for Raman sensing and (b) an extruded hollow core optical fiber used for Raman sensing of chemicals. In (a), the light is guided in the solid central triangular glass core and interacts with analytes in the surrounding voids. In (b), the situation is reversed, with the light propagating through the central void (surrounded by a thin suspended glass ring), where it overlaps with the sample.

(SCFs).⁶⁵ In this geometry, a light-guiding glass core is surrounded by a number of air-voids that can be filled with a liquid sample [Fig. 5(a)].⁷ The light from the core extends into the sample areas due to the small diameter of the core in comparison to the wavelength of light used, leading to the enhancement of the Raman signal coming from the sample along the entire length of the fiber, and therefore high signal visibility.⁶ This geometry was successfully shown to be able to measure low concentrations of organic molecules in liquids by uniquely identifying and quantifying them in solution, with limits of detection down to sub-microgram amounts in small sampling volumes (60 nL).⁶⁶

An alternative approach to Raman fiber sensing relies again on increased interaction lengths between the fiber and the sample, but reverses the geometry, guiding most of the light in a void surrounded by glass, as shown in Fig. 5(b). This single suspended ring hollow core optical fiber geometry is based on antiresonance reflection optical waveguiding (ARROW), combining a capillary-like total internal reflection guidance modified by Fabry-Perot interference in the thin ($<1 \mu\text{m}$) walls of the suspended ring. The target sample is then loaded in the central void and its signature collected from the proximal end of the fiber. This fiber geometry has been shown to offer a significant improvement in signal visibility in comparison to bulk volume sensing. An increase in the signal-to-noise ratio in comparison to solid-core optical fiber Raman sensors was obtained due to the large overlap between the guided light and the sample being interrogated.²¹ Further development of optical fibers for Raman spectroscopy can combine these techniques with advanced approaches such as resonant Raman scattering, which has been used to quantify the concentration of vitamin B12 in human blood over 15-82 μM .⁶⁷

E. Fluorescent chemical sensing with optical fibers

Fluorescence is an important sensing modality which is highly compatible with optical fibers. Fluorescent chemical sensing using optical fibers can be performed with small molecular fluorescent chemosensors attached to the fiber surface.^{9,68} The chemosensors are excited along the fiber so that the excitation can be delivered to otherwise inaccessible locations in the body.¹⁸ The fluorescence signal is then collected via the same fiber. Optical fiber-based chemical sensors and biosensors can detect a wide range of analytes including gases, ions, pollutants, agrochemicals, drugs, and pharmaceuticals, as well as biologically relevant molecules such as glucose; see Refs. 5, 69, and 70.

Different strategies have been used to functionalize fiber cores with chemosensors, such as covalently attaching silanes,⁶⁸ physical attachment of charged polymers (polyelectrolytes),⁷¹ thin-film deposition of doped polymers,⁹ or introducing functional groups on the fiber surface with surface linking chemistry.⁷² Using this approach, biologically significant ions such as Ca^{2+} , Zn^{2+} , Cd^{2+} , and Al^{3+} can be sensed and quantified.^{8,15,23,71} Variants of these surface bound chemosensors can be switched on and off, using light at a wavelength different from the excitation light. This allows

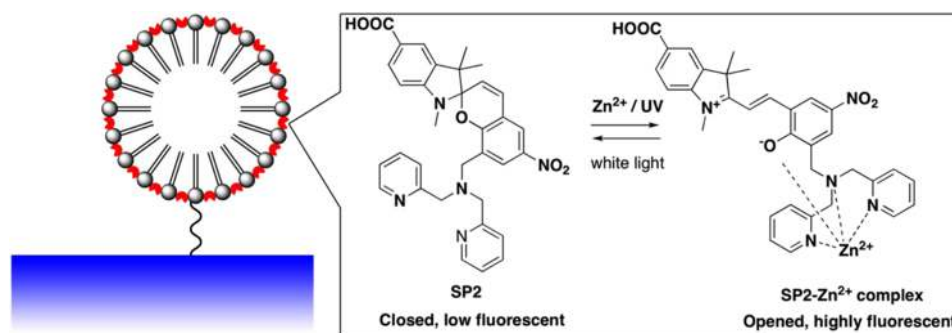


FIG. 6. Schematic of the optical fiber-based sensing architecture where a photoswitchable spiropyran chemosensor (SP2, red) is embedded within a liposome (gray). This structure (SP2-liposome) is covalently attached to the surface of an ECF or SCF (blue). The inset shows the isomeric structures of spiropyran SP2 (closed, nonfluorescent spiropyran isomer) and the metal-induced ring-opened Zn²⁺ complex (opened, fluorescent merocyanine isomer). Reproduced with permission from Heng *et al.*, ACS Appl. Mater. Interfaces **8**(20), 12727 (2016). Copyright 2016 Author(s), licensed under a Creative Commons Attribution 4.0 License.

repeatable sensing of metal ions using the same fiber without reinsertion,^{8,23,68} which is particularly attractive for *in vivo* studies.

Microstructured optical fibers (MOFs) similar to those discussed in Sec. II D can also be used for fluorescence-based sensing. Similarly to the case of fluorescent fiber probes, the interaction between the light and chemical species extends along the entire length of the fiber.⁶ Alternatively, with exposed-core MOFs,⁷³ the suspended core is partly open to the environment, enabling easy access to the fiber core and removing the need for sample filling. A recent approach is to combine phospholipids with photochromic chemosensors to form a novel liposome-based switchable sensing material which is attached to the surface of MOFs,¹⁵ as shown in Fig. 6. These sensing liposomes can be readily made from a range of natural lipids and are nontoxic and biodegradable. Switching of the chemosensor enables multiple measurements on a single sample, without the requirement to change the sensor.¹⁵ The ability of this MOF/liposome platform to sense Zn²⁺ in pleural lavage and nasopharynx of mice was compared to that of established ion sensing methodologies such as inductively coupled plasma mass spectrometry (ICP-MS) and solution fluorescence based (FluoZin-3) methods. The MOF/liposome-based sensor provided comparable results with significant advantages by allowing the use of nanoliter sampling compared to ICP-MS (ml) and FluoZin-3 (μ l).¹⁵ The best achieved limit of detection for surface-attached chemosensors is 200 nM.⁷¹

F. Luminescent fiber probes sensing temperature in the brain

Local temperature sensing is highly important in physiology, and optical fiber sensing is particularly well suited to this task.⁴ The most common method used for optical fiber sensing of temperature is the inscription of Bragg gratings within the fiber core, which enables temperature to be tracked by monitoring the wavelength of light reflected from the grating.⁷⁴ This approach, however, is not ideal for biosensing applications as the gratings themselves are typically several millimeters to several centimeters long, limiting spatial resolution.⁴ Other resonant methods utilizing whispering gallery modes or Fabry-Perot cavities tend to also be sensitive to the environmental refractive index, requiring careful control over the experimental conditions to avoid artefacts.⁷⁵

Temperature measurement within the brain requires sub-millimeter accuracy and temperature resolution of less than 0.5 °C.¹⁸ To achieve these targets, we used rare earth thermometry, an approach where rare earth ions such as erbium or thulium are doped within a host medium such as crystal or glass.⁷⁶ These ions possess energy levels that are close enough that the populations within these levels markedly depend on small temperature changes near ambient temperature. For example, in erbium raising the environmental temperature increases the intensity of the 528 nm emission (from ²H_{11/2} → ⁴I_{15/2} transition) relative to the 548 nm emission (from ⁴S_{3/2} → ⁴I_{15/2} transition). Therefore, by

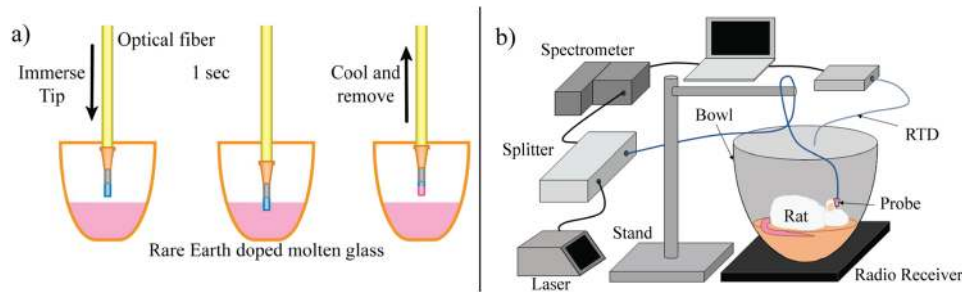


FIG. 7. (a) Coating of silica optical fiber tips with rare earth-doped tellurite glass. (b) Experimental setup for *in vivo* measurements to compare the brain and body temperature recordings in an ambulatory animal.¹⁸ Reprinted with permission from Musolino *et al.*, Biomedical Optics Express 7(8), 3069 (2016). Copyright 2016 Author(s), licensed under a Creative Commons Attribution 4.0 License.

monitoring the ratio of the emission signals from these two bands, the temperature can be determined with high accuracy (~ 0.1 K).¹⁰

For *in vivo* sensing, the temperature-sensitive rare earth ions must be mechanically integrated with an optical fiber, enabling spatially localized temperature sensing at specific discrete locations. We accomplished this by briefly immersing the tip of a conventional silica optical fiber into a molten glass doped with rare earth ions [Fig. 7(a)], which creates a thin film of glass on the fiber tip.^{10,20} This method combines the possibility of high doping concentrations and low phonon energy of the tellurite glass with robust, economical, and easy to integrate silica single mode fibers. Schartner and Monro examined the use of this sensor geometry utilizing bulk optics and characterized its behavior over the biologically relevant range from 23 to 39 °C.¹⁰ Here the total temperature-sensitive region of the fiber is less than 100 μm thick, with only the very end-face of the fiber contributing to the optical signal that is collected by the core for analysis. As such, this fiber is perfect for these *in vivo* sensing applications, allowing for the desired spatial resolution for biologically relevant measurements.

Musolino *et al.* extended on this work by using a compact, portable fiber-based configuration for coupling and collecting the upconversion emission signals, which greatly increased the stability of long-term measurements and allowed for its use within a conventional biological laboratory.¹⁸ This application demonstrated one of the key advantages of upconversion within a biological setting, in that, effectively, no autofluorescence is observed from the tissue, limiting any possible background interference of the optical signals. These probes were employed in measurements of brain temperature *in vivo* within the brain of ambulatory rats.¹⁸ Probes were inserted and monitored over an extended duration [Fig. 7(b)] to quantify changes to the brain temperature within the animals while they were able to move and behave freely.

G. Immunosensing of cytokines in the brain with optical fibers

Insertable optical fibers can enable *in vivo* biosensing on biologically relevant time scales even if their light-guiding function is not utilized, as the signal from the fiber surface can be simply collected by laser scanning microscopy. We have successfully developed such optical fiber-based immunosensors for monitoring of cytokines,^{2,17,30} where the conventional fiber readout was traded for the spatially localized cytokine detection. Cytokines are a diverse group of small proteins (10-70 kDa) involved in cellular signaling and also recognized as disease biomarkers.⁷⁷ The detection of cytokines is challenging because of their dynamic secretion process and low abundance *in vivo*, with physiological concentrations normally in the pM range.^{77,78}

Cytokine immunosensing in our approach was realized using highly specific antibody-antigen binding. The capture antibodies were immobilized on the surface of a decladded optical fiber (Fig. 8). Such a functionalized fiber was then incubated *in vivo* where it captured the cytokines. To visualize the cytokines, we used a “sandwich” approach; to this aim, the fiber was removed from the body, and

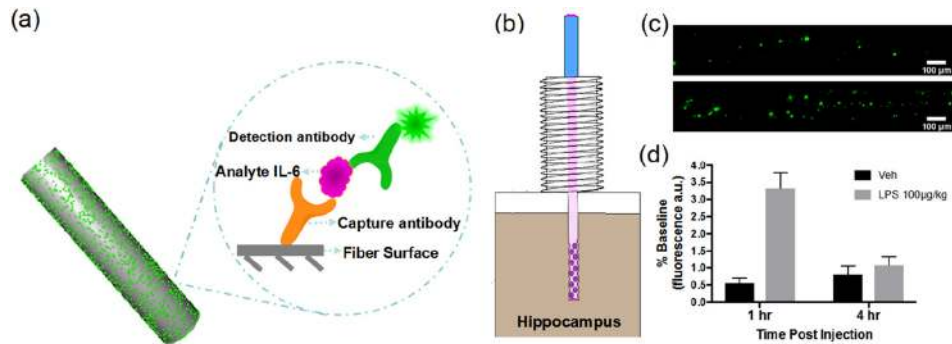


FIG. 8. (a) Schematic of the optical fiber sensing interface for Interleukin-6 (IL-6) detection. [(b)–(d)] *In vivo* detection of hippocampal IL-1 β release following peripheral lipopolysaccharide (LPS) administration: (b) Design of the IL-1 β sensing fiber with a perforated stainless-steel guide cannula. (c) Confocal z-stack maximum intensity projection images of optical fibers taken before (top) and 1 h after LPS administration (bottom). (d) Mean (\pm SEM) fluorescent signal expressed as the percentage of baseline of optical fibers following LPS or vehicle treatment ($n = 4$ –5 subjects/group; 1 fiber/subject at each time point). Reprinted with permission from Zhang *et al.*, *Brain, Behav., Immun.* **71**, 18 (2018). Copyright 2018 Author(s), licensed under a Creative Commons Attribution 4.0 License.²

fluorescent anti-cytokine detection antibodies were applied. These antibodies were labeled by very bright nanoparticles, which imparted high sensitivity to this assay.⁵³ The concentration of cytokines captured on the fiber surface was quantified by the integrated intensity of fluorescence measured by a microscope. This system has been successfully used for detection of IL-6 with the sensitivity of 0.4 pg ml^{-1} and spatial resolution in the order of $200 \text{ }\mu\text{m}$.³⁰ For comparison, a fiber sensor with conventional evanescent excitation and molecular fluorophores was able to detect IL-6 only to a concentration of 0.12 ng ml^{-1} , about 2 orders of magnitude lower than the physiologically relevant range.⁷⁹

To monitor spatially localized cytokine (IL-1 β) release in discrete brain regions, this fiber device was introduced into the brain through a perforated guide cannula with micrometer-sized holes drilled along its length to enable fluid exchange between the outside tissue and inside of the guide cannula [Fig. 8(b)]. The device demonstrated a physiologically relevant level of sensitivity of 3.9 pg ml^{-1} .² Upon the removal from the cannula, a new immunocapture device was then reintroduced for repeated analyte measurements *in vivo*, as shown in Figs. 8(c) and 8(d). This technology provides a sensing platform for *in vivo* monitoring of a spectrum of analytes in conscious, behaving animals.

III. IMAGING PLATFORMS

A. Optical coherence tomography (OCT)

OCT is a real-time optical imaging technique that utilizes low coherence interferometry to achieve high resolution (μm level) cross-sectional imaging.⁸⁰ Although the OCT's penetration depth is limited to only a few millimeters, it can be applied to deep tissue imaging with the aid of optical fiber probes.^{81,82} The typical spatial resolution achievable by a OCT fiber probe is 10 – $30 \text{ }\mu\text{m}$, which is suitable for many clinical applications, such as intraoperative guidance in arteries,^{83,84} reproductive tracts,⁸² and brain.²⁶

An OCT fiber probe is usually encased in either a flexible catheter or a rigid needle,⁸² which are commonly used in clinical settings. To enable access to solid tissues that are beyond the reach of catheters, OCT needle probes have been developed;³² these are mounted inside hypodermic needles. To date, the smallest side-viewing OCT probe can fit in a 30-gauge needle with an outer diameter of 0.31 mm [Fig. 9(a)].⁸⁵ This probe achieved a depth-of-field of $550 \text{ }\mu\text{m}$ with beam diameters below $30 \text{ }\mu\text{m}$. The highest system sensitivity achieved by a miniaturized OCT needle probe was reported at 112 dB , as illustrated in Figs. 9(b)–9(d).³³ This probe, which was encased in a 23-gauge needle (0.64 mm), is capable of lateral resolution of approximately $10 \text{ }\mu\text{m}$ at the focus. To match the size

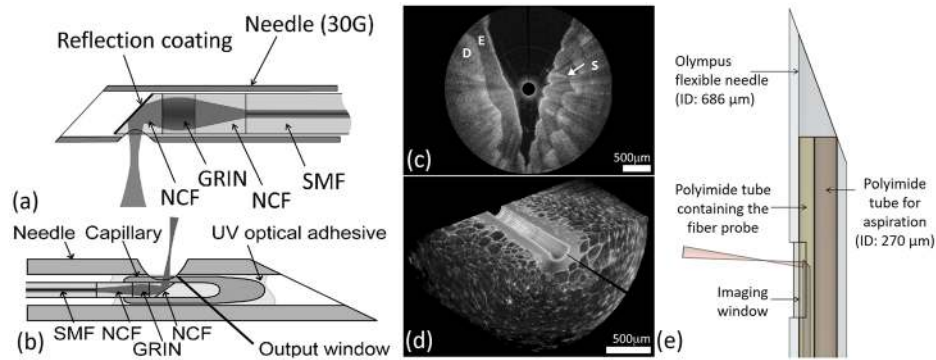


FIG. 9. OCT needle probes: (a) the design of a 30-gauge side-viewing OCT needle probe;⁸⁵ (b) the design of a high-sensitivity OCT needle probe;³³ [(c) and (d)] OCT images of a cucumber obtained with the high-sensitivity OCT needle probe; (e) the design of a flexible OCT needle probe which can simultaneously image and perform tissue aspiration.²⁴ Reprinted with permission from Lorensen *et al.*, *Opt. Lett.* **36**(19), 3894 (2011). Copyright 2011 Author(s), licensed under a Creative Commons Attribution 4.0 License; Scolaro *et al.*, *Opt. Lett.* **37**(24), 5247 (2012). Copyright 2012 Author(s), licensed under a Creative Commons Attribution 4.0 License; and Li *et al.*, *J. Biomed. Opt.* **22**(10), 106002 (2017). Copyright 2017 Author(s), licensed under a Creative Commons Attribution 4.0 License.

limitations of small surgical needles, both probes^{33,85} employed a graded-index (GRIN) fiber, with an outer diameter of 0.125 mm, to focus the OCT beam.

We recently developed a flexible version of these needle probes;²⁴ particularly useful for guiding biopsy or tissue aspiration in respiratory and gastrointestinal tracts. The probe uses a modified standard 19-gauge flexible needle (outer diameter 1.07 mm) and incorporates both a miniaturized OCT probe

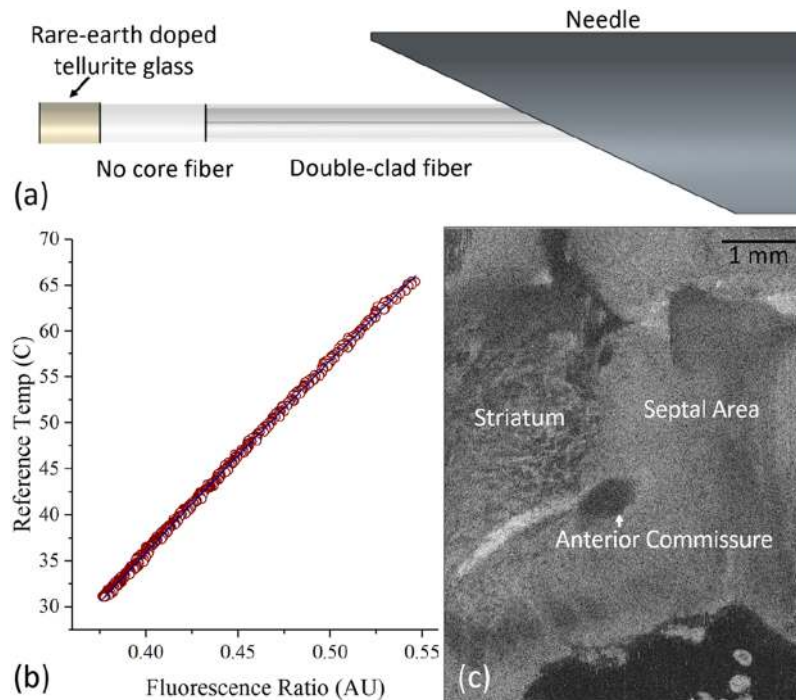


FIG. 10. Single-fiber-based imaging + sensing probe:²⁶ (a) Schematic of the distal tip of the imaging + sensing fiber probe; (b) fluorescence ratio obtained by the fiber probe vs. reference temperature for increasing temperature, $R^2 = 0.999$; (c) en-face OCT image obtained by the same probe in a rat brain. Visible structures include the striatum, anterior commissure, and septal area. Reprinted with permission from Li *et al.*, *Opt. Lett.* **43**(8), 1682 (2018). Copyright 2018 Author(s), licensed under a Creative Commons Attribution 4.0 License.

and a parallel channel to the aspirate tissue; see Fig. 9(e). This design facilitates accurate positioning of the needle tip relative to a lesion or lymph node.⁸⁶

Combining the OCT imaging with fiber sensing modalities mitigates the errors introduced by unguided sensing, where the probe might be inserted into a region of interest guided by only a standardized atlas.¹⁸ We were able to demonstrate that OCT imaging and (temperature) sensing functions can be integrated into a single-fiber-based probe.^{26,32} Similarly to combined fluorescence + OCT probes reported in Ref. 84, our temperature sensing + OCT probe utilizes a double-clad fiber (DCF) [Fig. 10(a)]. The single mode core of the DCF carries the OCT signal and excitation light for temperature sensing, and the multimode inner cladding collects the fluorescence emission light for temperature sensing. In this design, the temperature sensitive tellurite glass described in Sec. II F with refractive index $n = 1.98$ was used as a ball lens to focus light.⁸² This probe achieved lateral resolution of $18 \mu\text{m}$ at the focus. Similar approaches can be applied to simultaneous and spatially co-localized measurements of anatomical and physiological parameters such as pH and concentration of metal ions or small molecules.^{13,18,87}

B. Computational fiber bundle and multimode fiber imaging

Optical fiber bundles comprised of thousands of individual fiber cores in a cladding matrix are widely used in clinical microendoscopy.^{88,89} In this approach, the resolution is limited to the size of the individual fiber cores, with the resulting pixellation removed by postprocessing.⁹⁰ In the most simple systems, the distal facet is bare and must be placed nearly in contact with the sample. The resolution and contrast degrade rapidly away from the fiber facet plane because the shallow depth of field ($\sim 15 \mu\text{m}$) is set by the rather high numerical aperture (NA) of the fiber bundles (~ 0.4).

By considering the mode structure at the fiber bundle output, we devised a method to computationally increase the depth of field (Fig. 11).²⁷ Our approach is based on the idea that the prevalence of each mode depends on its angular coupling efficiency along with the amount of light entering the core at a given tilt angle.⁹¹ In typical few-mode fiber bundles, the oblique illumination tends to push light toward the periphery of the cores, whereas light entering normal to the fiber facet is localized to the center of the core [see Fig. 11(a)].²⁷ The effective collection aperture can therefore be reduced in post-processing to smaller angles by rejecting obliquely incident light which is located at the periphery of the cores at the output facet. As with any imaging device with an adjustable aperture, reducing the collection angle increases the depth of field, bringing previously blurred objects into focus [Fig. 11(b)]. This approach significantly increases the imaging distance of bare fiber bundles nearly to the working distance of lensed fiber bundles ($\sim 50 \mu\text{m}$). As a result, the imaging contrast

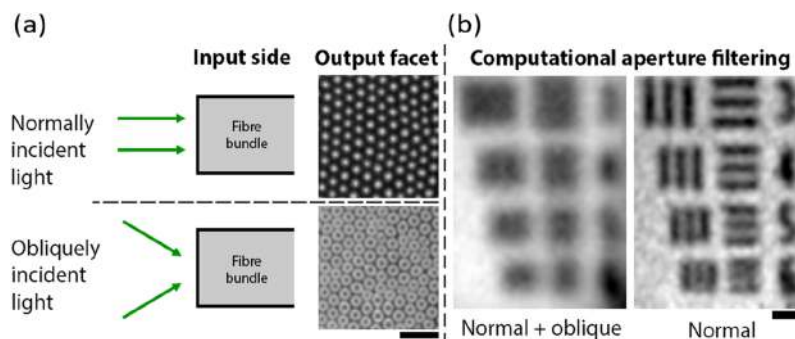


FIG. 11. (a) Top: Normally incident light on a fiber bundle input facet creates spots of light at the output facet, primarily composed of each core's fundamental mode. Bottom: Obliquely incident light creates rings of light at the output facet, pushing light toward the periphery of the cores. The scale bar is $10 \mu\text{m}$. (b) Left: Image of a USAF 1951 target (group 5, elements 3-6) at a distance of $70 \mu\text{m}$, through a lensless fiber bundle. This image is the result of standard processing, using both normal and obliquely incident light. (b) Right: By computationally subtracting oblique light, the aperture is effectively stopped down, extending the depth of field, thereby bringing the distant USAF target into focus. The scale bar is $50 \mu\text{m}$. Adapted from Orth *et al.* Opt. Express **26**(5), 6407 (2018). Copyright 2018 Author(s), licensed under a Creative Commons Attribution 4.0 License.

and resolution are substantially improved, especially for objects not in contact with the fiber facet. The technique is realized entirely computationally, avoiding scanning hardware modifications that increase the size and reduce the acquisition speed. Because the technique is incoherent, it could be implemented in existing fluorescence or reflection-based clinical microendoscopes without hardware modifications.

Despite the simplicity of this approach, it cannot enable imaging at arbitrary distances from the facet nor can it be used to fully shape excitation light. For the complete control of light through optical fibers, more sophisticated active feedback approaches are required.⁹²

The use of computational techniques plays a vital role in the new class of microendoscopes based on individual multimode fibers (MMFs) which have been recently identified as reliable optical elements for both light delivery and detection in imaging applications. The MMFs offer the highest resolution/footprint ratio of available endoscopes⁹³ with no need for miniaturisation as the MMFs are fabricated using established drawing techniques. Imaging through such fibers requires acquisition of complex light propagation characteristics, which are fully captured in the wavelength-dependent fiber transmission matrix. This approach views the MMF as a complete optical system. By careful calibration of the system, descrambling, and optical holography⁹² to select appropriate combinations of modes, scanner-free imaging can be achieved.⁹³ Although, in principle, fluorescence imaging is straightforward due to the point-like source of the emitter, in practice, this is complicated by the finite bandwidth of the emitter. The descrambling applied to one wavelength will typically vary across the fluorescence linewidth, which limits the amount of light that can be captured for fluorescence imaging in biological applications. In order to circumvent this issue, fluorescence imaging in MMF is realised by holographic-based raster-scanning of a focused point.⁹² The laser light is shaped by a hologram (determined by the fiber transmission matrix) and displayed on the spatial light modulator to produce a focal excitation spot in the desired position at the distal end of the fiber [Fig. 12(a)]. Light emitted from the excitation spot is then collected via the same fiber and detected at the proximal site [Fig. 12(b)] to produce an image of the fluorescent object [Fig. 12(c)].²⁹ Beside simple raster-scanning, the complete control of light in MMFs using computed holograms also enables advanced imaging modalities such as confocal,⁹⁴ two-photon,⁹⁵ and light-sheet.⁹⁶

The application of the above-mentioned methods for deep tissue imaging is limited by bending of the fiber, which changes the transmission matrix. Several computational approaches for bending compensation have been explored. These include adding a semi-transparent coating at the distal site of the fiber, which enables monitoring of reflected light and determination of the transmission matrix in real time.⁹⁷ A similar approach has been adopted by adding a reference beacon at the distal end of the fiber,⁹⁸ albeit with a limited bending range. The change in the transmission matrix can also be calculated theoretically if the current three-dimensional conformation of the fiber is monitored.⁹⁹ Future progress in this area will likely be driven by computational approaches which hold great promise for the future of microendoscopy and minimally invasive imaging in deep tissues of living organisms.

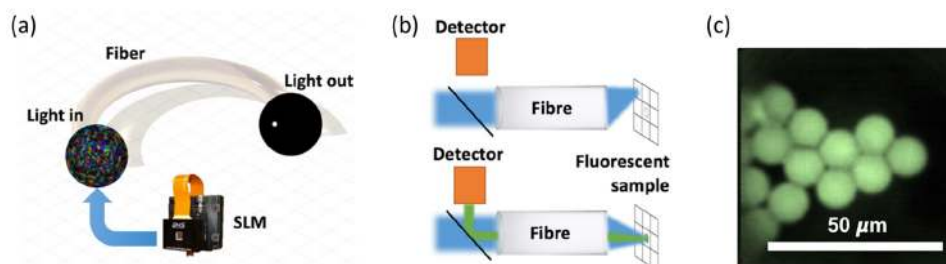


FIG. 12. (a) Hologram displayed on a spatial light modulator (SLM) creates an input light field that generates a focused spot at the fiber output. (b) Focused spot is raster-scanned over the fluorescent sample, and light emitted in places with fluorophores present is re-collected by the fiber and detected. (c) Image of $10\ \mu\text{m}$ size fluorescent spheres obtained by raster scanning of the focused spot at the distal site of MMFs.

IV. FUTURE OPPORTUNITIES

Bringing optical fiber sensing and imaging closer to real-life biological contexts requires specific adaptations spanning the areas of photonics and optical engineering, micro- and nanofabrication, materials science, nanotechnology, and chemistry. These provide opportunities for further development of fiber probes by increasing the signal to background ratio, tailoring the molecular components of the fiber probes, or multiplex sensing of different species and imaging on a single fiber (see Table I). We now discuss such potential future directions in more detail.

Increasing the signal to noise (or background) ratio is critical for rapid trace molecular analysis *in vivo*, especially when methods of chemical signal amplification cannot be applied. Fluorescence/luminescence signals can be enhanced by maximizing the photonic density of states at the sensing interfaces, achieved by refining the fiber geometry and related optical modes. Examples include the suspended and exposed core optical fibers discussed in Secs. II B, II D, and II E that aim to maximize the optical overlap between the sample and light,^{100,101} but much more can be achieved by yet unexplored designs. In the case of optical cavities written inside the fiber, the signal enhancement can also be achieved by increasing the reflectivity of the facets within the cavity and its Q-factor. The signal to noise ratio may also be improved by reducing the background

TABLE I. Promising approaches in the field of biomedical sensing and imaging fiber probes.

Challenges	Promising approaches that are yet to be fully explored
High background	<ol style="list-style-type: none"> 1. Maximize the photonic density of states at the sensing interfaces, through structuring of optical modes in microstructured fibers^{100,101} 2. Deposit tailored metal nanostructures in signal-generating areas of the optical fiber^{16,59} 3. Use upconverting particles so as to apply fluorescence excitation with a near-infrared light source which minimizes autofluorescence¹⁰ 4. Use time-gated or fluorescence-lifetime-based techniques to separate the signal and autofluorescence¹⁹ 5. Improve the design and fabrication of a microstructured fiber, such as a hollow core fiber, to reduce the overlap between the optical field and the background-generating parts of a fiber and thus minimize fiber fluorescence²¹
Low signals	<ol style="list-style-type: none"> 1. Utilize fluorescent signal amplification strategies¹⁰⁸ 2. Extend light-sample overlaps by utilizing the full fiber length instead of only the fiber tip⁶⁶ 3. Apply signal-enhancing structures and coatings¹⁶
Requirement for real-time measurements where signals follow variations in analyte levels	<ol style="list-style-type: none"> 1. Develop novel surface chemistry to optimize the sensing interface¹⁰⁹ 2. Integrate structure-switching based real-time sensors with optical fibers¹⁰²
Trade-off between the depth of focus and resolution in imaging	<ol style="list-style-type: none"> 1. Shape beams in a fiber-optic probe, e.g., create a Bessel beam that ensures both high resolution and large depth of focus^{96,110} 2. Use computational holography techniques by acquisition of complex light propagation characteristics and sophisticated active feedback using a spatial light modulator⁹²
Requirement for simultaneous sensing of multiple analytes	<ol style="list-style-type: none"> 1. Embed two or more fluorophores within a matrix located on the optical fiber¹³ 2. Exploit Raman or autofluorescence signatures of cells/tissues¹¹¹
Limited information obtained from a single modality	<ol style="list-style-type: none"> 1. Combine two or more imaging modalities into the same system⁸²⁻⁸⁴ 2. Integrate fiber sensing and imaging²⁶

contributions from the fiber itself. A particularly promising approach for Raman sensing is the use of hollow core optical fibers discussed in Sec. II D. The use of hollow cores reduces the overlap between the excitation light and the glass in the fiber that generates this background signature. Alternative approaches include fiber designs that separate the excitation and collection optical pathways, as is the case for the double clad fibers discussed in Sec. III A, or optimized optical fiber bundles combining new fiber geometries with discrete roles of multiple fibers within the bundle.

In addition to such structural modification, advancements in materials science may enable the deposition of tailored and designed metal nanostructures in signal-generating areas of the optical fiber (Sec. II C). Materials science also brings the capability to reduce the signal background, relevant in fluorescence, luminescence, and Raman sensing. For example, using infrared-excited upconverting labels strongly reduces the effect of autofluorescence background, both from the biological milieu and, critically, the fiber itself.

Finally, time-gated detection, whenever applicable, offers potential many orders of magnitude signal to noise improvements.¹⁹ This technique can increase the SNRs for ultrasmall analyte concentrations based on the differential temporal evolution of the target and background signals, and/or the location of targets relatively to the source and detector. Using time-gating will additionally allow us to clearly separate the instantaneous Raman signals from target analytes from slower-to-rise background signals of the glass impurities and, importantly, from overpowering biological autofluorescence signatures, allowing greater clarity of signature separation and lower detection limits.

Tailoring the molecular components of fiber probes offers further prospects for improved sensing performance. The molecular specificity in fiber sensing typically relies on specially coated surfaces incorporating molecular sensors, antibodies, or less temperature-sensitive aptamers able to selectively interact with specific targets. Identifiable light signatures are then generated upon target binding or with the aid of additional procedures. A common challenge with antibodies and particularly with aptamers is the reduction or loss of functionality upon surface binding; overcoming this problem will open the way for the fiber sensors to detect additional analytes.

Photoswitchable organic fluorophores engineered to respond to specific chemical species integrated with fibers yield sensing probes that are able to be regenerated by light and capable of repetitive measurements.^{15,23} This approach could be extended to new molecular targets, in particular, to small molecules. The normally off fluorescent FRET sensors integrated with optical fibers offer scope for *in vivo* sensing as their light signature can be produced *in vivo* upon target binding. They are well suited for the detection of selected macromolecules, allowing us to expand the range of analytes detectable by fiber sensors. The structure-switching real-time sensors¹⁰² when integrated with optical fibers will enable true real-time sensing required in longitudinal experiments. Finally, the approach of *in vivo* incubation of fiber probes followed by an external readout² realizes repetitive *in vivo* detection in a specific location in the body, but it still lends itself to traditional chemical amplification schemes and it offers the possibility of detecting a variety of targets. The above examples show that this area is at a really interesting disciplinary intersection, clearly poised for future growth.

Multiplexing sensing of different species and imaging on a single fiber is a common requirement in the life sciences. Most existing optical fiber sensors have been designed and optimized for single targets. While great scope exists to further develop these single-purpose devices, the greatest opportunity concerns creating multiplexed sensors that can act as “lab-on-a-fiber” devices for identifying and quantifying multiple chemical and biological species within a single sample and doing so at multiple locations.

To achieve this, work beyond refining individual sensing modalities is required, which creates a new and exciting range of potential developments. One could imagine, for example, a single microstructured fiber, with a structure optimized to increase light-sample interaction around its core, which also has multiple sensing areas just before its distal end, possibly a plasmonic sensor with antibodies to detect the accumulation of certain cells on the tip. This could be combined with obtaining a Raman signature through the same fiber to verify the cell type, while at the very tip of the fiber a GRIN lens could enable OCT observations to determine the environment and location in which

those cells were collected. Another option could be an exposed-core optical fiber that can perform multiple real-time (normally off) fluorescent assays at different locations along its length. Such a fiber probe could be implanted in living organisms for prolonged periods of time and interrogated periodically from the outside to monitor chemical responses to pain or medication. This could be perhaps accomplished using time-gated detection to offer localized information on where these events are happening along its length. Alternatively, such a spatially resolved readout along the fiber length could be realized using multiphoton techniques. Such an inert, light, and minimally invasive probe could be periodically read to determine physiological indicators such as the level of chronic pain in a patient. It is these truly disruptive uses of novel sensing and imaging optical fiber sensors as complete multiplexed systems that really stand to disrupt the landscape of photonic sensing in biomedical applications.

The flexible nature and the chemical-inertness of optical fiber probes make them well-suited for accessing physiological cavities and tubular structures, such as cardiovascular and reproductive systems and gastrointestinal, pulmonary, and urinary tracts.⁸² By detecting clinically relevant biomarkers and microstructures, the fiber probes are enabling improved diagnostic yield and/or intra-operative guidance.^{103,104} In the past 20 years, the clinical applications of fiber imaging probes in particular have grown at an accelerating pace, especially in diagnosing pre-malignant or early stage cancers to enable treatment at an early stage,⁸² and in achieving “smart,” microscopically targeted biopsies to minimize sampling errors.^{24,103} On the other hand, fiber sensing probes have so far been underutilized in medicine and have been mostly confined to high-cost niche applications in cardiology and neurology.¹⁰⁵ Thanks to the recent advances in optical communications and semiconductor technology, portable, robust, and inexpensive interrogation units are becoming available,^{87,106} opening up new possibilities to utilize biochemical optical fiber sensors. In addition, multidisciplinary research centers,¹⁰⁷ such as the Wellman Center for Photomedicine, the Beckman Laser Institute and Medical Clinic, the Medical Laser Center Lübeck, and the Centre for Nanoscale BioPhotonics, have created fertile environments for clinical translation of fiber sensors, environments where scientists communicate with clinicians to better understand their needs, allowing the targeted design of optical fiber devices that fit standard clinical workflows and can obtain regulatory approval.¹⁰⁴

V. CONCLUSION

In the past 5 years, the Centre for Nanoscale BioPhotonics has developed a suite of fiber probes for various applications in biological settings, including magnetic field sensing, chemical sensing of diverse analytes (ions, cytokines, vitamins, proteins, etc.), temperature sensing, and refractive index sensing and imaging (by single mode, multicore, or multimode fibers). These innovations have been realized via the convergence of multiple scientific disciplines and direct development based on the requirements of clinicians. Among many of the future development fronts, the following aspects are expected to benefit the most from the collaborative efforts between research areas: (1) improvement of the signal-to-background ratio; (2) customization of molecular sensors for fiber probes; (3) multiplexed sensing of different species; (4) single-fiber-based sensing and imaging; (5) clinical translation.

ACKNOWLEDGMENTS

This work is dedicated to Professor Tanya Monro, Deputy Vice-Chancellor Research at the University of South Australia, whose scientific vision has enabled pioneering research into fiber sensing. Her leadership of the successful Centre of Excellence bid has laid the foundations for the results presented in this paper. We are grateful for her ongoing support and engagement with the science program of the centre. The research presented here was partially supported by the Australian Research Council award (Nos. CE140100003 and FT160100357) and a Premier’s Research and Industry Fund grant provided by the South Australian Government Department of State Development. G.L. was funded by the Australian Research Council Future Fellowship. M.P. was funded by the Australian Research Council Discovery Early Career Researcher Award.

S.C.W.-S. was funded by a Ramsay Fellowship provided by the University of Adelaide. S.C.W.-S. was funded by the European Commission through the Seventh Framework Programme (FP7), No. PIFI-GA-2013-623248 (2015-2016). This work was performed in part at the Optofab node of the Australian National Fabrication Facility utilizing Commonwealth and South Australian State Government Funding. The authors acknowledge the Australian Defence Science and Technology Group (under the Signatures, Materials and Energy Corporate Enabling Research Program) for support of the silica suspended-core and exposed-core fiber development at The University of Adelaide.

- ¹ M. R. Hutchinson, "The importance of knowing you are sick: Nanoscale biophotonics for the 'other' brain," *Microelectron. Eng.* **187**, 101 (2018).
- ² K. Zhang, M. V. Baratta, G. Liu, M. G. Frank, N. R. Leslie, L. R. Watkins, S. F. Maier, M. R. Hutchinson, and E. M. Goldys, "A novel platform for *in vivo* detection of cytokine release within discrete brain regions," *Brain, Behav., Immun.* **71**, 18 (2018).
- ³ B. Culshaw, "Optical fiber sensor technologies: Opportunities and-perhaps-pitfalls," *J. Lightwave Technol.* **22**(1), 39 (2004).
- ⁴ B. Lee, "Review of the present status of optical fiber sensors," *Opt. Fiber Technol.* **9**(2), 57 (2003).
- ⁵ X.-d. Wang and O. S. Wolfbeis, "Fiber-optic chemical sensors and biosensors (2013–2015)," *Anal. Chem.* **88**(1), 203 (2015).
- ⁶ E. P. Schartner, G. Tsiminis, A. François, R. Kostecki, S. C. Warren-Smith, L. V. Nguyen, S. Heng, T. Reynolds, E. Klantsataya, K. J. Rowland, A. D. Abell, H. Ebdorff-Heidepriem, and T. M. Monroe, "Taming the light in microstructured optical fibers for sensing," *Int. J. Appl. Glass Sci.* **6**(3), 229 (2015).
- ⁷ T. M. Monroe, S. Warren-Smith, E. P. Schartner, A. François, S. Heng, H. Ebdorff-Heidepriem, and S. Afshar, "Sensing with suspended-core optical fibers," *Opt. Fiber Technol.* **16**(6), 343 (2010).
- ⁸ S. Heng, A. M. Mak, D. B. Stubing, T. M. Monroe, and A. D. Abell, "Dual sensor for Cd(II) and Ca(II): Selective nanoliter-scale sensing of metal ions," *Anal. Chem.* **86**(7), 3268 (2014).
- ⁹ R. Kostecki, H. Ebdorff-Heidepriem, S. Afshar V, G. McAdam, C. Davis, and T. M. Monroe, "Novel polymer functionalization method for exposed-core optical fiber," *Opt. Mater. Express* **4**(8), 1515 (2014).
- ¹⁰ E. P. Schartner and T. M. Monroe, "Fibre tip sensors for localised temperature sensing based on rare earth-doped glass coatings," *Sensors* **14**(11), 21693 (2014).
- ¹¹ A. François, T. Reynolds, and T. M. Monroe, "A fiber-tip label-free biological sensing platform: A practical approach toward *in-vivo* sensing," *Sensors* **15**(1), 1168 (2015).
- ¹² L. V. Nguyen, K. Hill, S. Warren-Smith, and T. Monroe, "Interferometric type optical biosensor based on exposed-core microstructured optical fiber," *Sens. Actuators, B* **221**, 320 (2015).
- ¹³ M. S. Purdey, J. G. Thompson, T. M. Monroe, A. D. Abell, and E. P. Schartner, "A dual sensor for pH and hydrogen peroxide using polymer-coated optical fibre tips," *Sensors* **15**(12), 31904 (2015).
- ¹⁴ Y. Ruan, H. Ji, B. C. Johnson, T. Ohshima, A. D. Greentree, B. C. Gibson, T. M. Monroe, and H. Ebdorff-Heidepriem, "Nanodiamond in tellurite glass Part II: Practical nanodiamond-doped fibers," *Opt. Mater. Express* **5**(1), 73 (2015).
- ¹⁵ S. Heng, C. A. McDevitt, R. Kostecki, J. R. Morey, B. A. Eijkelkamp, H. Ebdorff-Heidepriem, T. M. Monroe, and A. D. Abell, "Microstructured optical fiber-based biosensors: Reversible and nanoliter-scale measurement of Zinc ions," *ACS Appl. Mater. Interfaces* **8**(20), 12727 (2016).
- ¹⁶ P. Jia, Z. Yang, J. Yang, and H. Ebdorff-Heidepriem, "Quasiperiodic nanohole arrays on optical fibers as plasmonic sensors: Fabrication and sensitivity determination," *ACS Sens.* **1**(8), 1078 (2016).
- ¹⁷ G. Liu, K. Zhang, A. Nadort, M. R. Hutchinson, and E. M. Goldys, "Sensitive cytokine assay based on optical fiber allowing localized and spatially resolved detection of interleukin-6," *ACS Sens.* **2**(2), 218 (2016).
- ¹⁸ S. Musolino, E. P. Schartner, G. Tsiminis, A. Salem, T. M. Monroe, and M. R. Hutchinson, "Portable optical fiber probe for *in vivo* brain temperature measurements," *Biomedical Optics Express* **7**(8), 3069 (2016).
- ¹⁹ W. A. W. Razali, V. K. A. Sreenivasan, C. Bradac, M. Connor, E. M. Goldys, and A. V. Zvyagin, "Wide-field time-gated photoluminescence microscopy for fast ultrahigh-sensitivity imaging of photoluminescent probes," *J. Biophotonics* **9**(8), 848 (2016).
- ²⁰ E. P. Schartner, G. Tsiminis, M. R. Henderson, S. C. Warren-Smith, and T. M. Monroe, "Quantification of the fluorescence sensing performance of microstructured optical fibers compared to multi-mode fiber tips," *Opt. Express* **24**(16), 18541 (2016).
- ²¹ G. Tsiminis, K. J. Rowland, E. P. Schartner, N. A. Spooner, T. M. Monroe, and H. Ebdorff-Heidepriem, "Single-ring hollow core optical fibers made by glass billet extrusion for Raman sensing," *Opt. Express* **24**(6), 5911 (2016).
- ²² J. Zhao, X. Zheng, E. P. Schartner, P. Ionescu, R. Zhang, T. L. Nguyen, D. Jin, and H. Ebdorff-Heidepriem, "Upconversion nanocrystal-doped glass: A new paradigm for photonic materials," *Adv. Opt. Mater.* **4**(10), 1507 (2016).
- ²³ S. Heng, A. M. Mak, R. Kostecki, X. Zhang, J. Pei, D. B. Stubing, H. Ebdorff-Heidepriem, and A. D. Abell, "Photo-switchable calcium sensor: 'On'–'Off' sensing in cells or with microstructured optical fibers," *Sens. Actuators, B* **252**, 965 (2017).
- ²⁴ J. Li, B. C. Quirk, P. B. Noble, R. W. Kirk, D. D. Sampson, and R. A. McLaughlin, "Flexible needle with integrated coherence tomography probe for imaging during transbronchial tissue aspiration," *J. Biomed. Opt.* **22**(10), 106002 (2017).
- ²⁵ G. Tsiminis, E. P. Schartner, J. L. Brooks, and M. R. Hutchinson, "Measuring and tracking vitamin B12: A review of current methods with a focus on optical spectroscopy," *Appl. Spectrosc. Rev.* **52**(5), 439 (2017).
- ²⁶ J. Li, E. Schartner, S. Musolino, B. C. Quirk, R. W. Kirk, H. Ebdorff-Heidepriem, and R. A. McLaughlin, "Miniaturized single-fiber-based needle probe for combined imaging and sensing in deep tissue," *Opt. Lett.* **43**(8), 1682 (2018).

- ²⁷ A. Orth, M. Ploschner, I. S. Maksymov, and B. C. Gibson, "Extended depth of field imaging through multicore optical fibers," *Opt. Express* **26**(5), 6407 (2018).
- ²⁸ Y. Ruan, D. A. Simpson, J. Jeske, H. Ebendorff-Heidepriem, D. W. M. Lau, H. Ji, B. C. Johnson, T. Ohshima, S. Afshar, L. Hollenberg, A. D. Greentree, T. M. Monro, and B. C. Gibson, "Magnetically sensitive nanodiamond-doped tellurite glass fibers," *Sci. Rep.* **8**(1), 1268 (2018).
- ²⁹ S. A. Vasquez-Lopez, V. Koren, M. Ploschner, Z. Padamsey, T. Cizmar, and N. J. Emptage, "Minimally invasive deep-brain imaging through a 50 μm -core multimode fibre," *Light: Science and Applications* (published online).
- ³⁰ K. Zhang, G. Liu, and E. M. Goldys, "Robust immunosensing system based on biotin-streptavidin coupling for spatially localized femtogram mL^{-1} level detection of interleukin-6," *Biosens. Bioelectron.* **102**, 80 (2018).
- ³¹ M. Okada, N. I. Smith, A. F. Palonpon, H. Endo, S. Kawata, M. Sodeoka, and K. Fujita, "Label-free Raman observation of cytochrome c dynamics during apoptosis," *Proc. Natl. Acad. Sci. U. S. A.* **109** (1), 28 (2012).
- ³² R. A. McLaughlin, D. Lorensen, and D. D. Sampson, *Handbook of Coherent-Domain Optical Methods* (Springer, 2013), p. 1065.
- ³³ L. Scolaro, D. Lorensen, R. A. McLaughlin, B. C. Quirk, R. W. Kirk, and D. D. Sampson, "High-sensitivity anastigmatic imaging needle for optical coherence tomography," *Opt. Lett.* **37**(24), 5247 (2012).
- ³⁴ M. R. Henderson, B. C. Gibson, H. Ebendorff-Heidepriem, K. Kuan, V. Afshar, J. O. Orwa, I. Aharonovich, S. Tomljenovic-Hanic, A. D. Greentree, and S. Praver, "Diamond in tellurite glass: A new medium for quantum information," *Adv. Mater.* **23**(25), 2806 (2011).
- ³⁵ H. Ebendorff-Heidepriem, Y. Ruan, H. Ji, A. D. Greentree, B. C. Gibson, and T. M. Monro, "Nanodiamond in tellurite glass Part I: Origin of loss in nanodiamond-doped glass," *Opt. Mater. Express* **4**(12), 2608 (2014).
- ³⁶ D. Budker and M. Romalis, "Optical magnetometry," *Nat. Phys.* **3**(4), 227 (2007).
- ³⁷ B. M. Chernobrod and G. P. Berman, "Spin microscope based on optically detected magnetic resonance," *J. Appl. Phys.* **97**(1), 014903 (2005).
- ³⁸ F. Jelezko, T. Gaebel, I. Popa, A. Gruber, and J. Wrachtrup, "Observation of coherent oscillations in a single electron spin," *Phys. Rev. Lett.* **92**(7), 076401 (2004).
- ³⁹ T. M. Babinec, B. J. M. Hausmann, M. Khan, Y. Zhang, J. R. Maze, P. R. Hemmer, and M. Lončar, "A diamond nanowire single-photon source," *Nat. Nanotechnol.* **5**(3), 195 (2010).
- ⁴⁰ J. R. Rabeau, S. T. Huntington, A. D. Greentree, and S. Praver, "Diamond chemical-vapor deposition on optical fibers for fluorescence waveguiding," *Appl. Phys. Lett.* **86**(13), 134104 (2005).
- ⁴¹ T. Schröder, M. Fujiwara, T. Noda, H.-Q. Zhao, O. Benson, and S. Takeuchi, "A nanodiamond-tapered fiber system with high single-mode coupling efficiency," *Opt. Express* **20**(10), 10490 (2012).
- ⁴² I. V. Fedotov, L. V. Doronina-Amitonova, D. A. Sidorov-Biryukov, N. A. Safronov, S. Blakley, A. O. Levchenko, S. A. Zibrov, A. B. Fedotov, S. Y. Kilin, and M. O. Scully, "Fiber-optic magnetic-field imaging," *Opt. Lett.* **39**(24), 6954 (2014).
- ⁴³ T. Schroder, A. W. Schell, G. Kewes, T. Aichele, and O. Benson, "Fiber-integrated diamond-based single photon source," *Nano Lett.* **11**(1), 198 (2010).
- ⁴⁴ Y. Matsuzaki, H. Morishita, T. Shimooka, T. Tashima, K. Kakuyanagi, K. Semba, W. J. Munro, H. Yamaguchi, N. Mizuochi, and S. Saito, "Optically detected magnetic resonance of high-density ensemble of NV^- centers in diamond," *J. Phys.: Condens. Matter* **28** (27), 275302 (2016).
- ⁴⁵ S. Steinert, F. Dolde, P. Neumann, A. Aird, B. Naydenov, G. Balasubramanian, F. Jelezko, and J. Wrachtrup, "High sensitivity magnetic imaging using an array of spins in diamond," *Rev. Sci. Instrum.* **81**(4), 043705 (2010).
- ⁴⁶ X. Liu, J. Cui, F. Sun, X. Song, F. Feng, J. Wang, W. Zhu, L. Lou, and G. Wang, "Fiber-integrated diamond-based magnetometer," *Appl. Phys. Lett.* **103**(14), 143105 (2013).
- ⁴⁷ I. V. Fedotov, L. V. Doronina-Amitonova, D. A. Sidorov-Biryukov, N. A. Safronov, A. O. Levchenko, S. A. Zibrov, S. Blakley, H. Perez, A. V. Akimov, and A. B. Fedotov, "Fiber-optic magnetometry with randomly oriented spins," *Opt. Lett.* **39**(23), 6755 (2014).
- ⁴⁸ B. H. Lee, Y. H. Kim, K. S. Park, J. B. Eom, M. J. Kim, B. S. Rho, and H. Y. Choi, "Interferometric fiber optic sensors," *Sensors* **12**(3), 2467 (2012).
- ⁴⁹ X.-D. Fan, I. M. White, S. I. Shopova, H.-Y. Zhu, J. D. Suter, and Y.-Z. Sun, "Sensitive optical biosensors for unlabeled targets: A review," *Anal. Chim. Acta* **620**(1), 8 (2008).
- ⁵⁰ C. Caucheteur, T. Guo, and J. Albert, "Review of plasmonic fiber optic biochemical sensors: Improving the limit of detection," *Anal. Bioanal. Chem.* **407**(14), 3883 (2015).
- ⁵¹ S. C. Warren-Smith, R. M. André, J. Dellith, T. Eschrich, M. Becker, and H. Bartelt, "Sensing with ultra-short Fabry-Perot cavities written into optical micro-fibers," *Sens. Actuators, B* **244**, 1016 (2017).
- ⁵² S. C. Warren-Smith, R. M. André, C. Perrella, J. Dellith, and H. Bartelt, "Direct core structuring of microstructured optical fibers using focused ion beam milling," *Opt. Express* **24**(1), 378 (2016).
- ⁵³ R. M. André, S. C. Warren-Smith, M. Becker, J. Dellith, M. Rothhardt, M. I. Zibaii, H. Latifi, M. B. Marques, H. Bartelt, and O. Frazão, "Simultaneous measurement of temperature and refractive index using focused ion beam milled Fabry-Perot cavities in optical fiber micro-tips," *Opt. Express* **24**(13), 14053 (2016).
- ⁵⁴ E. Klantsataya, A. François, A. Zuber, V. Torok, R. Kostecki, and T. M. Monro, *Proc. SPIE* **8938**, 89380X (2014).
- ⁵⁵ G. Kostovski, P. R. Stoddart, and A. Mitchell, "The optical fiber tip: An inherently light-coupled microscopic platform for micro- and nanotechnologies," *Adv. Mater.* **26**(23), 3798 (2014).
- ⁵⁶ A. H. Heffernan, D. Stavrevski, I. Maksymov, R. Kostecki, H. Ebendorff-Heidepriem, A. D. Greentree, and B. C. Gibson, *Proc. SPIE* **10544**, 105440J (2018).
- ⁵⁷ D. J. Lipomi, R. V. Martinez, M. A. Kats, S. H. Kang, P. Kim, J. Aizenberg, F. Capasso, and G. M. Whitesides, "Patterning the tips of optical fibers with metallic nanostructures using nanoskiving," *Nano Lett.* **11**(2), 632 (2011).
- ⁵⁸ E. J. Smythe, M. D. Dickey, G. M. Whitesides, and F. Capasso, "A technique to transfer metallic nanoscale patterns to small and non-planar surfaces," *ACS Nano* **3**(1), 59 (2009).

- ⁵⁹ P. Jia and J. Yang, "A plasmonic optical fiber patterned by template transfer as a high-performance flexible nanoprobe for real-time biosensing," *Nanoscale* **6**(15), 8836 (2014).
- ⁶⁰ P. Jia, D. Kong, and H. Ebendorff-Heidepriem, "Direct optical fiber nanoimprint" (unpublished).
- ⁶¹ J. R. Ferraro, K. Nakamoto, and C. W. Brown, *Introductory Raman Spectroscopy*, 2nd ed. (Academic Press, 2003), p. 1.
- ⁶² C. Krafft and V. Sergo, "Biomedical applications of Raman and infrared spectroscopy to diagnose tissues," *Spectroscopy* **20**(5-6), 195 (2006).
- ⁶³ Z. Movasaghi, S. Rehman, and I. U. Rehman, "Raman spectroscopy of biological tissues," *Appl. Spectrosc. Rev.* **42**(5), 493 (2007).
- ⁶⁴ M. G. Shim, B. C. Wilson, E. Marple, and M. Wach, "Study of fiber-optic probes for *in vivo* medical Raman spectroscopy," *Appl. Spectrosc.* **53**(6), 619 (1999).
- ⁶⁵ H. Ebendorff-Heidepriem, S. C. Warren-Smith, and T. M. Monro, "Suspended nanowires: Fabrication, design and characterization of fibers with nanoscale cores," *Opt. Express* **17**(4), 2646 (2009).
- ⁶⁶ G. Tsiminis, F. Chu, S. C. Warren-Smith, N. A. Spooner, and T. M. Monro, "Identification and quantification of explosives in nanolitre solution volumes by Raman spectroscopy in suspended core optical fibers," *Sensors* **13**(10), 13163 (2013).
- ⁶⁷ G. Tsiminis, E. P. Schartner, J. L. Brooks, and M. R. Hutchinson, in *presented at the 2016 IEEE Photonics Conference (IPC)* (IEEE, 2016), p. 684.
- ⁶⁸ S. Heng, M.-C. Nguyen, R. Kostecki, T. M. Monro, and A. D. Abell, "Nanoliter-scale, regenerable ion sensor: Sensing with a surface functionalized microstructured optical fibre," *RSC Adv.* **3**(22), 8308 (2013).
- ⁶⁹ H. H. Qazi, A. B. b. Mohammad, and M. Akram, "Recent progress in optical chemical sensors," *Sensors* **12**(12), 16522 (2012).
- ⁷⁰ M. Pospíšilová, G. Kuncová, and J. Trögl, "Fiber-optic chemical sensors and fiber-optic bio-sensors," *Sensors* **15**(10), 25208 (2015).
- ⁷¹ S. C. Warren-Smith, S. Heng, H. Ebendorff-Heidepriem, A. D. Abell, and T. M. Monro, "Fluorescence-based aluminum ion sensing using a surface-functionalized microstructured optical fiber," *Langmuir* **27**(9), 5680 (2011).
- ⁷² R. Kostecki, S. Heng, H. Ebendorff-Heidepriem, A. D. Abell, and T. M. Monro, *Proc. SPIE* **9157**, 915788 (2014).
- ⁷³ R. Kostecki, H. Ebendorff-Heidepriem, C. Davis, G. McAdam, S. C. Warren-Smith, and T. M. Monro, "Silica exposed-core microstructured optical fibers," *Opt. Mater. Express* **2**(11), 1538 (2012).
- ⁷⁴ S. W. James, M. L. Dockney, and R. P. Tatam, "Simultaneous independent temperature and strain measurement using in-fibre Bragg grating sensors," *Electron. Lett.* **32**(12), 1133 (1996).
- ⁷⁵ S. H. Nam and S. Yin, "High-temperature sensing using whispering gallery mode resonance in bent optical fibers," *IEEE Photonics Technol. Lett.* **17**(11), 2391 (2005).
- ⁷⁶ S. A. Wade, S. F. Collins, and G. W. Baxter, "Fluorescence intensity ratio technique for optical fiber point temperature sensing," *J. Appl. Phys.* **94** (8), 4743 (2003).
- ⁷⁷ G. Scapigliati, F. Buonocore, and M. Mazzini, "Biological activity of cytokines: An evolutionary perspective," *Curr. Pharm. Des.* **12**(24), 3071 (2006).
- ⁷⁸ G. Liu, M. Qi, M. R. Hutchinson, G. Yang, and E. M. Goldys, "Recent advances in cytokine detection by immunosensing," *Biosens. Bioelectron.* **79**, 810 (2016).
- ⁷⁹ R. Kapoor and C.-W. Wang, "Highly specific detection of interleukin-6 (IL-6) protein using combination tapered fiber-optic biosensor dip-probe," *Biosens. Bioelectron.* **24**(8), 2696 (2009).
- ⁸⁰ D. Huang, E. A. Swanson, C. P. Lin, J. S. Schuman, W. G. Stinson, W. Chang, M. R. Hee, T. Flotte, K. Gregory, and C. A. Puliafito, "Optical coherence tomography," *Science* **254**(5035), 1178 (1991).
- ⁸¹ E. A. Swanson and J. G. Fujimoto, "The ecosystem that powered the translation of OCT from fundamental research to clinical and commercial impact," *Biomed. Opt. Express* **8**(3), 1638 (2017).
- ⁸² M. J. Gora, M. J. Suter, G. J. Tearney, and X. Li, "Endoscopic optical coherence tomography: Technologies and clinical applications," *Biomed. Opt. Express* **8**(5), 2405 (2017).
- ⁸³ J. Li, X. Li, D. Mohar, A. Raney, J. Jing, J. Zhang, A. Johnston, S. Liang, T. Ma, K. K. Shung, S. Mahon, M. Brenner, J. Narula, Q. Zhou, P. M. Patel, and Z. Chen, "Integrated IVUS-OCT for real-time imaging of coronary atherosclerosis," *Jt. Assess. Commod. Chem.: Cardiovasc. Imaging* **7**(1), 101 (2014).
- ⁸⁴ H. Yoo, J. W. Kim, M. Shishkov, E. Namati, T. Morse, R. Shubochkin, J. R. McCarthy, V. Ntziachristos, B. E. Bouma, F. A. Jaffer, and G. J. Tearney, "Intra-arterial catheter for simultaneous microstructural and molecular imaging *in vivo*," *Nat. Med.* **17**, 1680 (2011).
- ⁸⁵ D. Lorensen, X. Yang, R. W. Kirk, B. C. Quirk, R. A. McLaughlin, and D. D. Sampson, "Ultrathin side-viewing needle probe for optical coherence tomography," *Opt. Lett.* **36**(19), 3894 (2011).
- ⁸⁶ L. P. Harii, M. Mino-Kenudson, E. J. Mark, and M. J. Suter, "*In vivo* optical coherence tomography: The role of the pathologist," *Arch. Pathol. Lab. Med.* **136**(12), 1492 (2012).
- ⁸⁷ E. P. Schartner, M. R. Henderson, M. Purdey, D. Dhattrak, T. M. Monro, P. G. Gill, and D. F. Callen, "Cancer detection in human tissue samples using a fiber-tip pH probe," *Cancer Res.* **76**(23), 6795 (2016).
- ⁸⁸ M. Hughes, T. P. Chang, and G.-Z. Yang, "Fiber bundle endocytoscopy," *Biomed. Opt. Express* **4**(12), 2781 (2013).
- ⁸⁹ J. M. Jabbour, M. A. Saldia, J. N. Bixler, and K. C. Maitland, "Confocal endomicroscopy: Instrumentation and medical applications," *Ann. Biomed. Eng.* **40**(2), 378 (2011).
- ⁹⁰ F. Taleblou and C. Depeursinge, U.S. patent 5878159 A (2 March 1999).
- ⁹¹ A. W. Snyder and J. Love, *Optical Waveguide Theory* (Springer Science & Business Media, 1983), p. 734.
- ⁹² T. Čížmár and K. Dholakia, "Exploiting multimode waveguides for pure fibre-based imaging," *Nat. Commun.* **3**, 1027 (2012).
- ⁹³ Y. Choi, C. Yoon, M. Kim, T. D. Yang, C. Fang-Yen, R. R. Dasari, K. J. Lee, and W. Choi, "Scanner-free and wide-field endoscopic imaging by using a single multimode optical fiber," *Phys. Rev. Lett.* **109**(20), 203901 (2012).
- ⁹⁴ D. Loterie, S. Farahi, I. Papadopoulos, A. Goy, D. Psaltis, and C. Moser, "Digital confocal microscopy through a multimode fiber," *Opt. Express* **23**(18), 23845 (2015).

- ⁹⁵ E. E. Morales-Delgado, D. Psaltis, and C. Moser, "Two-photon imaging through a multimode fiber," *Opt. Express* **23**(25), 32158 (2015).
- ⁹⁶ M. Plöschner, V. Kollárová, Z. Dostál, J. Nylk, T. Barton-Owen, D. E. K. Ferrier, R. Chmelfk, K. Dholakia, and T. Čižmár, "Multimode fibre: Light-sheet microscopy at the tip of a needle," *Sci. Rep.* **5**, 18050 (2015).
- ⁹⁷ R. Y. Gu, R. N. Mahalati, and J. M. Kahn, "Design of flexible multi-mode fiber endoscope," *Opt. Express* **23**, 26905 (2015).
- ⁹⁸ S. Farahi, D. Ziegler, I. N. Papadopoulos, D. Psaltis, and C. Moser, "Dynamic bending compensation while focusing through a multimode fiber," *Opt. Express* **21**(19), 22504 (2013).
- ⁹⁹ M. Plöschner, T. Tyc, and T. Čižmár, "Seeing through chaos in multimode fibres," *Nat. Photonics* **9**(8), 529 (2015).
- ¹⁰⁰ S. C. Warren-Smith, S. Afshar, and T. M. Monro, "Fluorescence-based sensing with optical nanowires: A generalized model and experimental validation," *Opt. Express* **18**(9), 9474 (2010).
- ¹⁰¹ V. S. Afshar, S. C. Warren-Smith, and T. M. Monro, "Enhancement of fluorescence-based sensing using microstructured optical fibres," *Opt. Express* **15**(26), 17891 (2007).
- ¹⁰² C. Cao, F. Zhang, E. M. Goldys, and G. Liu, "Advances in structure-switching aptasensing towards real time detection of cytokines," *TrAC, Trends Anal. Chem.* **102**, 379 (2018).
- ¹⁰³ M. Goetz, N. P. Malek, and R. Kiesslich, "Microscopic imaging in endoscopy: Endomicroscopy and endocytoscopy," *Nat. Rev. Gastroenterol. Hepatol.* **11**(1), 11 (2014).
- ¹⁰⁴ R. Correia, S. James, S. W. Lee, S. P. Morgan, and S. Korposh, "Biomedical application of optical fibre sensors," *J. Opt.* **20**(7), 073003 (2018).
- ¹⁰⁵ É. Pinet, "Medical applications: Saving lives," *Nat. Photonics* **2**(3), 150 (2008).
- ¹⁰⁶ S. P. Singh, O. Ibrahim, H. J. Byrne, J. W. Mikkonen, A. P. Koistinen, A. M. Kullaa, and F. M. Lyng, "Recent advances in optical diagnosis of oral cancers: Review and future perspectives," *Head Neck* **38**(S1), E2403 (2016).
- ¹⁰⁷ B. J. Tromberg, R. R. Anderson, R. Birngruber, R. Brinkmann, M. W. Berns, J. A. Parrish, and G. Apiou-Sbirlea, "Biomedical optics centers: Forty years of multidisciplinary clinical translation for improving human health," *J. Biomed. Opt.* **21**(12), 124001 (2016).
- ¹⁰⁸ M. E. Tanenbaum, L. A. Gilbert, L. S. Qi, J. S. Weissman, and R. D. Vale, "A protein-tagging system for signal amplification in gene expression and fluorescence imaging," *Cell* **159**(3), 635 (2014).
- ¹⁰⁹ C. Cao, Y. Zhang, C. Jiang, M. Qi, and G. Liu, "Advances on aryldiazonium salt chemistry based interfacial fabrication for sensing applications," *ACS Appl. Mater. Interfaces* **9**(6), 5031 (2017).
- ¹¹⁰ K. M. Tan, M. Mazilu, T. H. Chow, W. M. Lee, K. Taguchi, B. K. Ng, W. Sibbett, C. S. Herrington, C. T. A. Brown, and K. Dholakia, "In-fiber common-path optical coherence tomography using a conical-tip fiber," *Opt. Express* **17**(4), 2375 (2009).
- ¹¹¹ D. Fu, F.-K. Lu, X. Zhang, C. Freudiger, D. R. Pernik, G. Holtom, and X. S. Xie, "Quantitative chemical imaging with multiplex stimulated Raman scattering microscopy," *J. Am. Chem. Soc.* **134**(8), 3623 (2012).